ELSEVIER

Journal of Alloys and Compounds 303–304 (2000) 445–453

Journal of ALLOYS AND COMPOUNDS

www.elsevier.com/locate/jallcom

Syntheses, crystal structures, and thermal behavior of the rare earth amidosulfates $M(NH_2SO_3)_3 \cdot 2H_2O$ (M=Pr, Nd, Sm)

Mathias S. Wickleder

Institut für Anorganische Chemie, Universität zu Köln, D-50939 Köln, Germany

Abstract

Evaporation of solutions of M^{3+} (M=Pr, Nd, Sm) in aqueous amidosulfonic acid leads to the amidosulfate dihydrates $M(NH_2SO_3)_3 \cdot 2H_2O$. According to X-ray single crystal structure determinations, they contain eight-fold-coordinate M^{3+} ions with the $[MO_8]$ polyhedra and amidosulfate groups connected to infinite sheets which are held together via hydrogen bridges. DTA/TG investigations show that the dihydrates lose H_2O in a two-step mechanism yielding amidosulfate monohydrates as intermediates. The anhydrous amidosulfates decompose in two steps to the anhydrous sulfates, $M_2(SO_4)_3$ (M=Pr–Sm). The decomposition of these compounds has been confirmed by means of temperature-dependent X-ray powder diffraction. By very slow dehydration under flowing argon, single crystals of the monohydrate intermediate for M=Sm were obtained. This triclinic compound has a layer structure and contains eight-fold-coordinate Sm^{3+}. However, the $NH_2SO_3^-$ ions are higher coordinated than is the corresponding dihydrate. Further heating yields the anhydrous amidosulfates as crystalline powders. According to the X-ray investigations, they are isotypic with $La(NH_2SO_3)_3$. The structure of the latter can be considered a derivative of the UCl_3-type of structure with complex anions.

Keywords: Lanthanides; Amidosulfates; Thermal behavior

1. Introduction

Anhydrous rare earth compounds with complex anions such as NO_3^-, SO_4^{2-} or ClO_4^- have been rarely investigated, because single crystals suitable for X-ray investigations are hard to obtain. Due to the thermal lability of the substances, crystals cannot be grown from a melt, and from solutions one always gets compounds containing solvent molecules. However, it has been recently shown for $Eu(ClO_4)_3$ that single crystals can be prepared by dehydration of $Eu(ClO_4)_3 \cdot 6H_2O$ under special conditions [1]. Furthermore, intermediate phases in the dehydration process like $Lu(ClO_4)_3 \cdot 3H_2O$ and $M(ClO_4)_3 \cdot H_2O$ (M=Er,Yb) could be obtained in single crystal form by careful temperature adjustment [2,3].

The crystal structure determination of $Eu(ClO_4)_3$ revealed that the compound crystallizes with the same structure as the hydrogensulfates of the lighter rare earth elements $M(HSO_4)_3$ (M=La–Eu) [4]. The additional proton in the latter has no influence on the crystal structure, so hydrogen bonding seems to be negligible. In this context structural investigations of the rare earth amidosulfates (sulfamates) seemed to be interesting. The $NH_2SO_3^-$ ion can be derived from the HSO_4^- (=$HOSO_3^-$) ion by substitution of NH_2 for OH, resulting in the introduction of an additional H atom. If the possibility of hydrogen bonding has no influence on the crystal structure, then isotypy to the respective hydrogensulfates would be expected.

Amidosulfates of the rare earth elements can be obtained from aqueous solutions of the respective oxides in amidosulfonic acid as hydrates [5]. Because even the hydrates are not characterized the first step was to determine their structure. Subsequently, the thermal behavior of the compounds should be studied in order to get information on how to synthesize the anhydrous species and, if necessary, intermediate phases.

2. Experimental

For the syntheses of $M(NH_2SO_3)_3 \cdot 2H_2O$ (M=Pr, Nd, Sm), the respective oxides M_2O_3 (M=Nd, Sm) (Aldrich, 99.9) and $Pr_2(CO_3)_2 \cdot xH_2O$ (Strem, 99.9) were dissolved in separate solutions of NH_3SO_3 (Merck, p.a.) until neutrality was achieved. Upon evaporation at 60°C, single

E-mail address: mathias.wickleder@uni-koeln.de (M.S. Wickleder)

0925-8388/00/$ – see front matter
PII: S0925-8388(00)00624-1

crystals of the dihydrates were obtained. These are light green for M=Pr, violet for M=Nd and light yellow for M=Sm. For the preparation of $Sm(NH_2SO_3)_3 \cdot H_2O$, the respective dihydrate was transferred to a silica boat which was placed in a silica tube (d=60 mm). The tube was put in a resistance furnace and purged with dry argon. The furnace was slowly heated to 150°C (5°C/h). The product obtained was essentially a light yellow powder which contained single crystals suitable for X-ray diffraction measurements. $Sm(NH_2SO_3)_3 \cdot H_2O$ is moisture sensitive and was handled in a glove box in an argon atmosphere. For all compounds studied in this work, small crystals of about 0.1 mm in diameter were sealed in glass capillaries for X-ray analysis. The scattering intensities were collected with an Imaging-plate-diffractometer (Stoe and Cie). The measurement of the $Sm(NH_2SO_3)_3 \cdot 2H_2O$ crystal was carried out at 150 K. Structure solution and refinement were carried out using the programs SHELXS86 and SHELXL93 [6,7]. An absorption correction was applied using the program DIFABS [8]. H atom positions were taken from the difference Fourier card at the end of the refinement. The positional parameters were not refined. For $Nd(NH_2SO_3)_3 \cdot 2H_2O$ the H positions resulting from the refinement of the corresponding praseodymium compound were used. The displacement parameters of the H atoms were fixed in the case of $Sm(NH_2SO_3)_3 \cdot H_2O$ The data collection parameters and the determined crystallographic data are given in Tables 1–6. Further details of the crystal structure determinations are available from the Fachinformationszentrum Karlsruhe, D–76344 Eggenstein–Leopoldshafen, Germany, on quoting the depository numbers CSD 410897 ($Pr(NH_2SO_3)_3 \cdot 2H_2O$), CSD 410898 ($Nd(NH_2SO_3)_3 \cdot 2H_2O$), CSD 410899 ($Sm(NH_2SO_3)_3 \cdot 2H_2O$), and CSD 410900 ($Sm(NH_2SO_3)_3 \cdot H_2O$), respectively.

DTA/TG investigations were performed using a STA 409 thermal analyzer (Netzsch). For that purpose about 20 mg of the substances were filled in corundum containers and heated at a constant rate of 10 K/min under flowing argon. The thermal decomposition was followed from 30°C up to 800°C. For the DTA data a baseline correction was applied. Onset and end temperatures of the thermal effects were taken from the differentiated DTA curve following common procedures using the software supplied with the analyzer [9].

Temperature-dependent powder diffraction data were collected using a powder diffractometer (Stoe and Cie) equipped with a position sensitive detector and a graphite

Table 1
Data collection parameters and crystal data for $M(NH_2SO_3)_3 \cdot 2H_2O$ [M=Pr (1), Nd (2), Sm (3)] and $Sm(NH_2SO_3)_3 \cdot H_2O$ (4)

Lattice parameters (Å, °)	**1:** a=7.9214(10)	**2:** a=7.89.80(13)	**3:** a=7.8240(14)	**4:** a=6.815(1)
	b=9.1435(12)	b=9.1138(15)	b=9.068(2)	b=9.397(1)
	c=9.2541(12)	c=9.2177(15)	c=9.1641(15)	c=9.431(2)
	α=117.69(1)	α=117.59(1)	α=117.61(2)	α=68.06(2)
	β=95.18(1)	β=95.25(2)	β=95.11(2)	β=75.30(2)
	γ=92.25(1)	γ=92.24(2)	γ=92.10(2)	γ=83.34(2)
Molar volume (cm^3/mol)	177.3	175.6.1	172.1	163.1
No. of formula units, Z		2		
Crystal system		Triclinic		
Space group		*P-1* (ITC No.2)		
Diffractometer		Stoe IPDS		
Radiation		Mo–K_α (graphite monochromator, λ=0.7107 Å)		
Temperature (K)	293	293	150	293
Data range	6° <2θ<52°	6°<2θ<52°	6°<2θ<52°	6°<2θ<50°
Index range	−10≤h≤10	−10≤h≤10	−9≤h≤9	−7≤h≤7
	−12≤k≤12	−12≤k≤12	−11≤k≤10	−9≤k≤10
	−12≤l≤12	−12≤l≤12	−10≤l≤10	−10≤l≤10
Rotation angle range; φ-increment	0°<φ<200°; 2°	0°<φ<200°; 2°	0°<φ<250°; 2°	0°<φ<250°; 2
No. of images	100	100	125	125
Exposure time (min)	4	6	4	8
Detector distance (mm)	60	60	60	60
Data corrections		Polarization/Lorentz		
Absorption corrections		DIFABS [8]		
μ (cm^{-1})	47.3	50.5	57.4	60.5
No. of collected reflections	5702	5544	6770	
No. of unique reflections	2182	2155	2073	1443
No. of reflections with I_o>2σ(I)	1986	1766	2031	1203
R_{int}	0.0348	0.0407	0.0227	0.0359
Structure determination		F99 SHELXS-86 and SHELXS-93 [6,7]		
Scattering factors		Intern. Tables, Vol. C		
Goodness of fit	1.000	1.058	1.104	0.888
R1; wR2 I_o>2σ(I)	0.0213; 0.0487	0.0313; 0.0671	0.0155; 0.0402	0.0318; 0.0652
R1; wR2 (all data)	0.0250; 0.0495	0.0461; 0.0699	0.0162; 0.0404	0.0418; 0.0674

Table 2
Positional parameters and equivalent isotropic displacement parameters for $M(NH_2SO_3)_3 \cdot 2H_2O$

Atom[a]	*x*/*a*			*y*/*b*			*z*/*c*			$U_{eq} \cdot 10^{-1}/pm^2$ [b]		
	Pr	Nd	Sm	Pr	Nd	Sm	Pr	Nd	Sm	Pr	Nd	Sm
M	0.21944(2)	0.21950(5)	0.22016(2)	0.38040(2)	0.38071(5)	0.38029(1)	0.21802(2)	0.21800(4)	0.21733(1)	8.98(7)	9.8(1)	3.31(6)
S1	0.3957(1)	0.3969(2)	0.39642(9)	0.3216(1)	0.3218(2)	0.32222(8)	0.5853(1)	0.5851(2)	0.58383(7)	13.0(2)	13.2(4)	5.5(1)
O11	0.4834(4)	0.4838(8)	0.4878(3)	0.1828(4)	0.1817(7)	0.1827(3)	0.5725(4)	0.5720(7)	0.5726(3)	32.9(7)	33.0(1)	15.3(5)
O12	0.5076(4)	0.5062(7)	0.5059(3)	0.5178(4)	0.5183(7)	0.5149(3)	0.3153(3)	0.3148(6)	0.3178(2)	26.7(7)	26.0(1)	11.9(4)
O13	0.3294(4)	0.3310(7)	0.3278(3)	0.2985(3)	0.2994(6)	0.2967(3)	0.4237(3)	0.4222(5)	0.4199(2)	21.7(6)	20.0(1)	9.6(4)
N1	0.2376(4)	0.2354(8)	0.2357(3)	0.3310(5)	0.3310(9)	0.3333(3)	0.6898(4)	0.6892(7)	0.6914(3)	23.5(8)	22.0(2)	10.5(5)
H111	0.1972	0.1972	0.2005	0.4111	0.4111	0.4364	0.7186	0.7186	0.7382	25.0(14)[c]	11.0(23)	11.0(8)
H112	0.1656	0.1656	0.1521	0.2524	0.2524	0.2600	0.6380	0.6380	0.6358	48.0(17)	26.0(23)	24.0(10)
S2	0.8559(1)	0.8556(2)	0.85676(9)	0.2783(1)	0.2787(2)	0.27877(8)	0.8940(1)	0.8954(2)	0.89501(1)	11.6(2)	11.8(4)	4.6(1)
O21	0.0190(3)	0.0188(6)	0.0237(3)	0.2525(3)	0.2529(6)	0.2526(2)	0.9583(3)	0.9587(3)	0.9589(2)	16.3(6)	17.0(1)	7.3(4)
O22	0.7305(4)	0.7298(6)	0.7311(3)	0.3239(3)	0.3243(7)	0.3258(3)	0.0076(4)	0.0088(6)	0.0122(2)	25.2(7)	25.0(1)	10.6(4)
O23	0.1234(4)	0.1239(7)	0.1247(3)	0.6059(3)	0.6045(6)	0.6053(2)	0.1724(3)	0.1720(6)	0.1745(2)	22.3(6)	22.0(1)	9.5(4)
N2	0.7849(4)	0.7850(8)	0.7852(3)	0.0945(4)	0.0942(7)	0.0930(3)	0.7444(4)	0.7444(6)	0.7452(3)	19.2(7)	17.0(1)	8.1(5)
H211	0.7054	0.7054	0.6876	0.1050	0.1050	0.0972	0.6802	0.6802	0.6721	10.0(10)	18.0(21)	18.0(9)
H212	0.8644	0.8644	0.8521	0.0431	0.0431	0.0388	0.6993	0.6993	0.6734	44.0(16)	30.0(24)	27.0(10)
S3	0.1369(1)	0.1360(2)	0.13481(9)	0.7639(1)	0.7631(2)	0.76110(8)	0.6203(1)	0.6201(2)	0.61957(7)	12.8(2)	12.8(4)	5.3(1)
O31	0.0679(4)	0.0678(7)	0.0638(3)	0.8780(3)	0.8765(7)	0.8751(3)	0.5695(3)	0.5684(6)	0.5657(2)	26.5(7)	27.0(1)	11.4(4)
O32	0.1740(4)	0.1752(7)	0.1733(3)	0.6099(3)	0.6088(6)	0.6039(2)	0.4841(3)	0.4845(6)	0.4832(2)	25.9(7)	25.0(1)	10.7(4)
O33	0.9652(4)	0.9659(6)	0.9669(3)	0.2703(4)	0.2724(7)	0.2712(3)	0.2737(3)	0.2736(6)	0.2707(2)	25.5(7)	25.0(1)	10.9(4)
N3	0.3141(5)	0.3132(9)	0.3151(3)	0.8594(5)	0.8609(9)	0.8603(3)	0.7398(4)	0.7406(8)	0.7389(3)	27.9(9)	25.0(2)	11.5(5)
H311	0.3647	0.3647	0.3639	0.8109	0.8109	0.7894	0.7619	0.7619	0.7879	99.0(34)	32.0(34)	41.0(12)
H312	0.3765	0.3765	0.4085	0.9005	0.9005	0.8842	0.6922	0.6922	0.6682	45.0(15)	36.0(25)	75.0(18)
O1	0.2940(4)	0.2932(7)	0.2948(3)	0.0940(3)	0.0965(6)	0.0967(2)	0.0910(3)	0.0910(6)	0.0898(2)	27.0(7)	27.0(1)	11.6(4)
H11	0.2962	0.2962	0.2937	0.0437	0.0437	0.0433	0.0031	0.0031	0.0009	14.0(11)	6.0(18)	13.0(9)
H12	0.2758	0.2758	0.2741	0.0369	0.0369	0.0358	0.1289	0.1289	0.1285	46.0(17)	54.0(33)	48.0(14)
O2	0.3760(4)	0.3763(7)	0.3756(3)	0.3282(4)	0.3293(7)	0.3346(3)	0.9830(4)	0.9853(6)	0.9867(2)	26.8(7)	26.0(1)	11.6(4)
H21	0.4719	0.4719	0.4678	0.3384	0.3384	0.3378	0.9891	0.9891	0.9893	43.0(17)	44.0(32)	13.0(10)
H22	0.3373	0.3373	0.3351	0.3319	0.3319	0.3308	0.9052	0.9052	0.9035	48.0(19)	15.0(20)	24.0(10)

[a] All atoms occupy the site 2*i* of space group *P-1*.
[b] $U_{eq} = 1/3[U_{11}(aa^*)^2 + U_{22}(bb^*)^2 + U_{33}(cc^*)^2 + 2U_{12}aba^*b^*\cos\gamma + 2U_{13}aca^*c^*\cos\beta + 2U_{23}bcb^*c^*\cos\alpha]$ [13].
[c] Isotropic displacement parameter for H atoms.

Table 3
Positional parameters and equivalent displacement parameters for $Sm(NH_2SO_3)_3 \cdot H_2O$

Atom[a]	x/a	y/b	z/c	$U_{eq}^{-}10^{-1}/pm^{2}$ [b]
Sm	0.13282(7)	0.18535(6)	0.07967(6)	10.6(2)
S1	0.3065(3)	0.7835(3)	0.0923(3)	11.4(6)
O11	0.2341(10)	0.9159(9)	0.1339(8)	25.6(2)
O12	0.5014(9)	0.1934(9)	0.0199(7)	19(2)
O13	0.1590(9)	0.7295(9)	0.0382(8)	23(2)
N1	0.3180(11)	0.6510(10)	0.2570(9)	19(2)
H111[c]	0.3993	0.5575	0.2445	50[d]
H112	0.3661	0.6782	0.3044	50
S2	0.2520(3)	0.1132(3)	0.6953(3)	11.8(5)
O21	0.4593(9)	0.1221(8)	0.6095(7)	20(2)
O22	0.1610(9)	0.9696(8)	0.7327(8)	25(2)
O23	0.2309(10	0.1524(9)	0.8318(7)	28(2)
N2	0.1294(11)	0.2408(9)	0.5708(8)	17(2)
H211	0.9954	0.2735	0.6200	50
H212	0.1678	0.3008	0.4600	50
S3	0.7821(3)	0.4367(3)	0.2432(3)	13.0(6)
O31	0.7551(10)	0.4807(9)	0.3770(8)	26(2)
O32	0.7848(9)	0.5630(8)	0.0950(7)	18(2)
O33	0.9590(9)	0.3358(8)	0.2287(7)	16(2)
N3	0.5752(10)	0.3455(10	0.2732(9)	17(2)
H311	0.5874	0.3030	0.1954	50
H312	0.5027	0.2881	0.3647	50
O1	0.2355(9)	0.1025(9)	0.3249(7)	26(2)
H11	0.3159	0.0252	0.3502	50
H12	0.1550	0.1425	0.4031	50

[a] All atoms occupy the site 2*i* of space group *P-1*.
[b] $U_{eq} = 1/3[U_{11}(aa^*)^2 + U_{22}(bb^*)^2 + U_{33}(cc^*)^2 + 2U_{12}aba^*b^*\cos\gamma + 2U_{13}aca^*c^*\cos\beta + 2U_{23}bcb^*c^*\cos\alpha]$ [13].
[c] Positions of H atoms from difference Fourier card, not refined.
[d] Fixed isotropic displacement parameters for all H atoms.

Table 4
Selected internuclear distances (Å) in $M(NH_2SO_3)_3 \cdot 2H_2O$

	Pr	Nd	Sm
M–O33	2.418(2)	2.398(5)	2.371(2)
–O23	2.425(3)	2.403(5)	2.382(2)
–O12	2.440(3)	2.422(5)	2.394(2)
–O1	2.444(3)	2.419(5)	2.401(2)
–O32	2.452(2)	2.442(5)	2.412(2)
–O13	2.453(3)	2.431(5)	2.409(1)
–O2	2.463(3)	2.440(5)	2.401(5)
–O21	2.494(3)	2.483(4)	2.447(2)
S1–O11	1.433(3)	1.438(6)	1.442(2)
–O13	1.454(3)	1.458(5)	1.457(2)
–O12	1.455(3)	1.452(5)	1.462(2)
–N1	1.631(3)	1.641(6)	1.643(3)
S2–O22	1.439(3)	1.445(5)	1.448(2)
–O21	1.450(3)	1.441(5)	1.456(2)
–O23	1.462(3)	1.464(5)	1.469(2)
–N2	1.637(3)	1.638(5)	1.639(2)
S3–O31	1.435(3)	1.428(6)	1.445(2)
–O32	1.453(3)	1.453(5)	1.460(2)
–O33	1.454(3)	1.459(3)	1.459(2)
–N3	1.641(4)	1.640(4)	1.648(3)

furnace. The finely powdered samples were sealed in silica capillaries (diameter=0.3 mm) with grease (Apiezon L). Data were collected in Debye–Scherrer geometry in the range of $2\theta = 7°–60°$ at 30°C and from 100 to 500°C at 50°C intervals. After each heating period the system was allowed to equilibrate for 30 min. The data were processed applying smoothing and background corrections in the program package VISUAL X-POW (Stoe and Cie) [10]. With the help of the same program, lattice parameter refinements based on least-square procedures were performed.

3. Results and discussion

3.1. Crystal structures

The amidosulfate dihydrates $M(NH_2SO_3)_3 \cdot 2H_2O$ (M= Pr, Nd, Sm) crystallize in the triclinic crystal system, space group *P-1* (No. 2). The structure is now described for $Pr(NH_2SO_3)_3 \cdot 2H_2O$. Pr^{3+} is eight-fold coordinated by oxygen atoms. The coordination polyhedron can be viewed as a distorted square antiprism (Fig. 1). The oxygen ligands belong to six $NH_2SO_3^-$ groups and two H_2O molecules. The three crystallographically different

Table 5
Distances (Å) and angles (°) of hydrogen bonds in the compounds $M(NH_2SO_3)_3 \cdot 2H_2O$

D–H···A[a]	H–D			H···A			D–A			Angle at H		
	Pr	Nd	Sm	Pr	Nd	Sm	Pr	Nd	Sm	Pr	Nd	Sm
N1–H111–O22	0.75	0.74	0.90	2.56	2.54	2.30	3.08	3.06	3.01	128	129	135
–O23				2.84	2.83	2.80	3.20	3.18	3.14	112	111	104
N1–H112–O31	0.82	0.80	0.85	2.36	2.35	2.23	3.10	3.06	3.03	149	149	157
N2–H211–O11	0.86	0.86	0.98	2.24	2.23	2.09	3.09	3.07	3.04	166	166	162
N2–H212–O31	0.83	0.82	0.85	2.28	2.28	2.24	3.10	3.09	3.05	174	174	157
N3–H311–O1	0.70	0.70	1.01	2.82	2.82	2.77	2.97	2.96	2.95	124	125	109
N3–H312–O11	0.87	0.87	1.09	2.58	2.56	2.24	3.30	3.30	3.23	142	143	150
O1–H11–N3	0.73	0.73	0.73	2.25	2.23	2.22	2.97	2.96	2.95	172	174	172
O1–H12–N2	0.77	0.78	0.80	2.10	2.09	2.06	2.87	2.87	2.85	173	172	173
O2–H21–O22	0.76	0.75	0.72	2.06	2.04	2.06	2.80	2.79	2.78	169	169	172
O2–H22–N1	0.77	0.79	0.79	2.07	2.07	2.04	2.85	2.86	2.83	177	178	177

[a] D=donor, A=acceptor.

Table 6
Selected internuclear distances (Å) and angles (°) in $Sm(NH_2SO_3)_3 \cdot H_2O$

Sm–O32	2.355(7)	S1–O11	1.438(7)
–O33	2.373(6)	–O13	1.440(7)
–O23	2.389(6)	–O12	1.449(6)
–O1	2.407(5)	–N1	1.601(8)
–O13	2.433(5)		
–O12	2.434(6)	S2–O21	1.433(6)
–O11	2.441(7)	–O22	1.435(8)
–O22	2.493(7)	–O23	1.436(6)
		–N2	1.652(7)
		S3–O31	1.432(7)
		–O32	1.454(7)
		–O33	1.456(6)
		–N3	1.643(8)

Hydrogen bonding (D: donor, A: acceptor)

D–H···A	H–D	H···A	D–A	Angle at H
N1–H111–N3	101	217	316	167
N1–H112–O21	74	278	349	159
N2–H211–N1	99	233	331	178
N2–H212–O33	97	280	347	128
–N3		287		126
N3–H311–O12	94	246	337	162
N3–H312–O21	88	222	304	155
O1–H11–O21	85	195	280	169
O1–H12–N2	97	208	296	152

amidosulfate groups are bonded via oxygen atoms to two further Pr^{3+} ions according to $Pr(H_2O)_2(NH_2SO_3)_{6/2}$. The linkage of the $[PrO_8]$ polyhedra and $NH_2SO_3^-$ tetrahedra occurs only in two dimensions, leading to sheets which are connected via hydrogen bonds (Fig. 1) involving the donor atoms O1 and N2 and the acceptor atoms N3, N2 and O31, respectively. Additionally hydrogen bonds are observed within the sheets involving the donor atoms N1 and O2 and the acceptor atoms O22 and N1, respectively. Further hydrogen bonds as well as bond lengths and angles, are summarized in Table 5.

In the crystal structure of $Sm(NH_2SO_3)_3 \cdot H_2O$, also triclinic, space group *P-1*, Sm^{3+} is surrounded by seven $NH_2SO_3^-$ groups and one water molecule. Coordination number eight is retained from the dihydrate, although the compound contains only one H_2O molecule. This is achieved by a higher connectivity of one of the three crystallographically different amidosulfate groups which links three Sm^{3+} ions with each other according to $Sm(H_2O)(NH_2SO_3)_{3/3}(NH_2SO_3)_{4/2}$. Note that the stronger connectivity of this $NH_2SO_3^-$ group remarkably influences the S–N distance which is only 1.6 Å now (Table 6). In spite of the stronger polyhedra linkage, $Sm(NH_2SO_3)_3 \cdot H_2O$ still adopts a layer structure similar to that of the dihydrate (Fig. 2). Again, the sheets are held together via hydrogen bonding with O1 and N3 as donors and N2 as well as O21 as acceptors. Details of these and the additionally observed hydrogen bonds are given in Table 6.

The anhydrous amidosulfates $M(NH_2SO_3)_3$ (M=Pr–Sm) crystallize isotypic with $La(NH_2SO_3)_3$ with a structure that can be considered a UCl_3-type of structure with complex anions [11]. In the crystal structure, M^{3+} ions are surrounded by nine oxygen atoms in the form of a tricapped trigonal prism. The oxygen atoms belong to nine $NH_2SO_3^-$ groups, each of which is attached to two further M^{3+} ions according to $M(NH_2SO_3)_{9/3}$. The tricapped trigonal prisms form rods along the [001] which are shifted by $1/2c$ with respect to each other (Fig. 3). The rods are stacked in a hexagonal fashion thereby forming channels

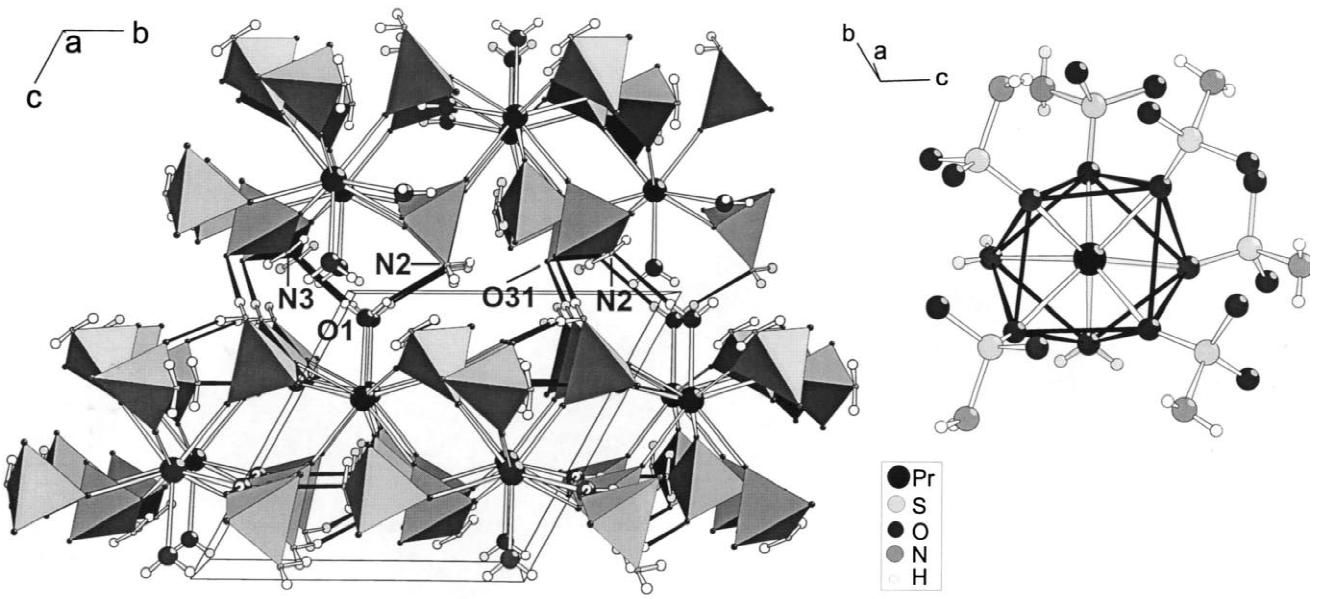

Fig. 1. Perspective view of the crystal structure of $Pr(NH_2SO_3)_3 \cdot 2H_2O$; hydrogen bonds are emphasized in black; the $[Pr(NH_2SO_3)_6(H_2O)_2]$ complex is additionally shown on the right.

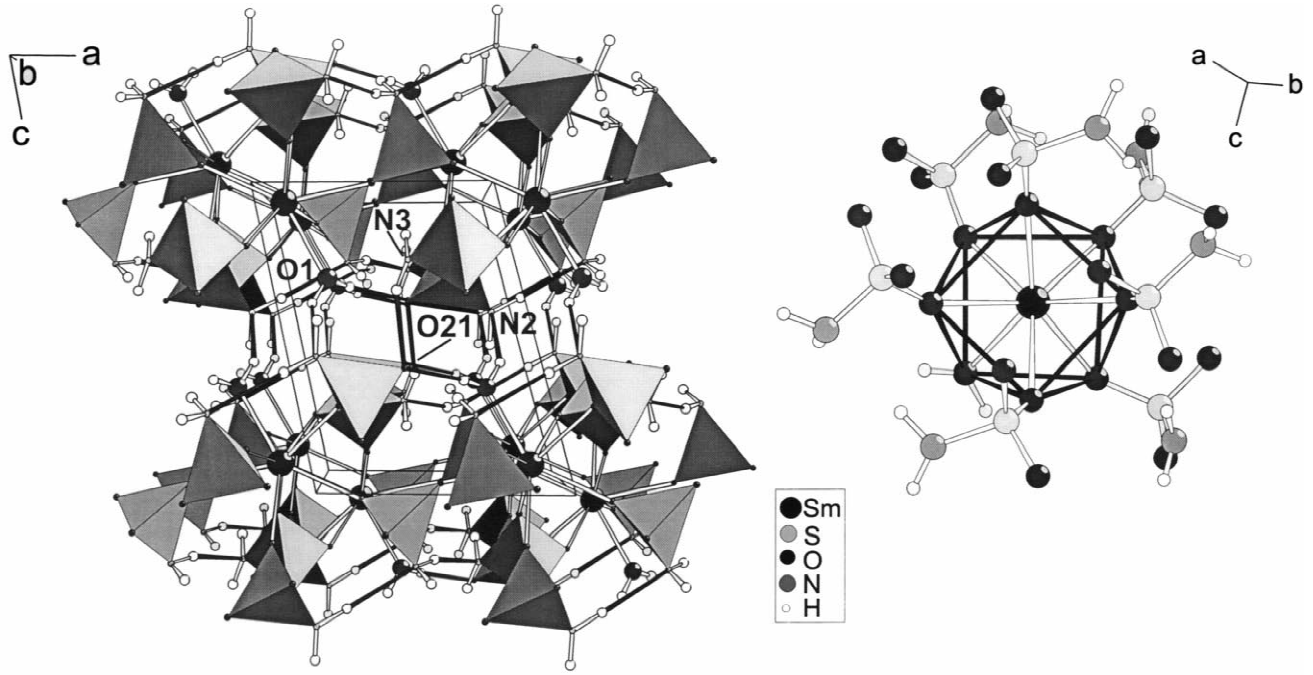

Fig. 2. Perspective view of the crystal structure of $Sm(NH_2SO_3)_3 \cdot H_2O$; hydrogen bonds are emphasized in black; the $[Sm(NH_2SO_3)_7(H_2O)]$ complex is additionally shown on the right.

parallel to the [001] direction. The NH_2 groups in the $NH_2SO_3^-$ ions are oriented toward these channels. This same structure is found for the respective perchlorates and hydrogensulfates. In accordance with the original expectation, the additional hydrogen atoms seem to have no influence on the crystal structure.

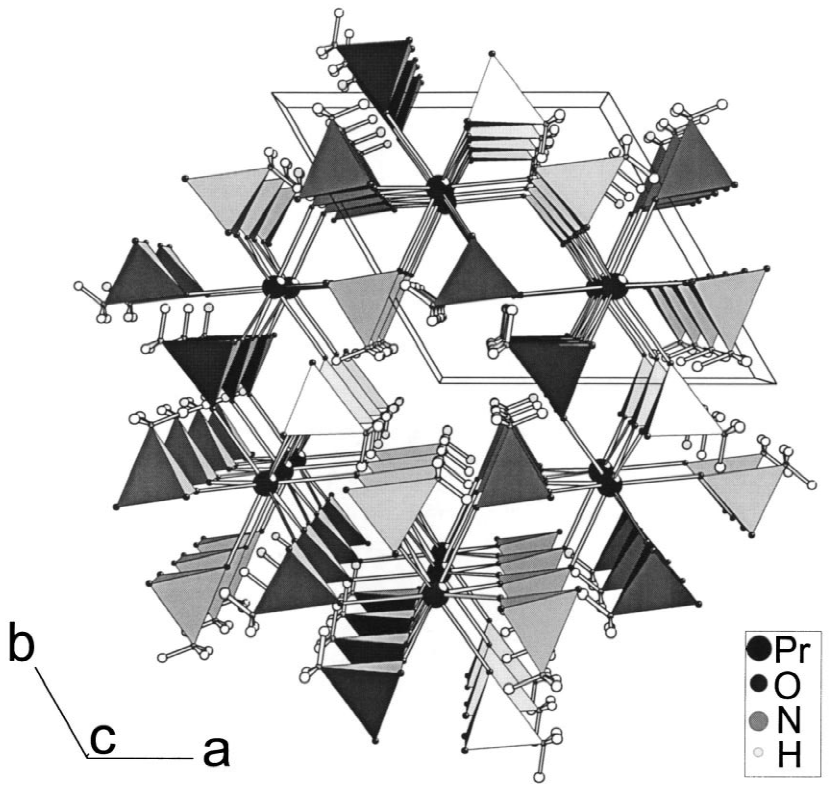

Fig. 3. Perspective view of the crystal structure of $Pr(NH_2SO_3)_3$ along [001]; note that all NH_2 groups point toward the channels parallel to the projection direction.

Table 7
Results of the thermal decomposition of $Pr(NH_2SO_3)_3 \cdot 2H_2O$ (DTA/TG data)

Reaction	T_{onset} (°C)	T_{end} (°C)	T_{max} (°C)	Mass loss (observed)/%	Mass loss (calcd.)/%
$Pr(NH_2SO_3)_3 \cdot 2H_2O \rightarrow Pr(NH_2SO_3)_3 \cdot H_2O$	119.7		138.6	3.8	3.9
$Pr(NH_2SO_3)_3 \cdot H_2O \xrightarrow{-H_2O} Pr(NH_2SO_3)_3$		209.8	177.9	3.9	3.8
$Pr(NH_2SO_3)_3 \xrightarrow{-H_2O} \rightarrow$	319.3	351.8	327.4	24.8	33.3
$\rightarrow r2(SO_4)_3$	439.3	461.7	446.0	5.6	33.3
				Σ 38.1	Σ 41.0

Table 8
Results of the thermal decomposition of $Sm(NH_2SO_3)_3 \cdot 2H_2O$ (DTA/TG data)

Reaction	T_{onset} (°C)	T_{end} (°C)	T_{max} (°C)	Mass loss/% (observed)	Mass loss/% (calcd.)
$Sm(NH_2SO_3)_3 \cdot 2H_2O \rightarrow Sm(NH_2SO_3)_3 \cdot H_2O$	145.9		169.2	3.8	3.8
$Sm(NH_2SO_3)_3 \cdot H_2O \xrightarrow[-H_2O]{-H_2O} Sm(NH_2SO_3)_3$		242.6	226.9	3.3	3.6
$Sm(NH_2SO_3)_3 \rightarrow$	327.2	357.5	335.1	16.3	30.3
$\rightarrow Sm(SO_4)_3$	419.5	453.8	435.1	13.6	30.3
				Σ 37.0	Σ 37.7

3.2. Thermal behavior

The thermal behavior of the amidosulfates has been investigated by means of DTA/TG measurements for $Pr(NH_2SO_3)_3 \cdot 2H_2O$ and $Sm(NH_2SO_3)_3 \cdot 2H_2O$ (Tables 7 and 8, Fig. 4). The dehydration of $Pr(NH_2SO_3)_3 \cdot 2H_2O$ starts at 120°C and follows a two-step mechanism yielding a monohydrate as an intermediate. The final formation of $Pr_2(SO_4)_3$ is accompanied by two exothermic steps at 327 and 446°C with mass losses of 24.8 and 5.6%, respectively. $Sm(NH_2SO_3)_3 \cdot 2H_2O$ dehydrates also in a two-step process but at a higher temperature and with the onset at 146°C. Compared to the praseodymium compound, the peaks correlated to the dehydration steps are more separated. The peak maxima are 139 and 178°C for the praseodymium amidosulfate, 169 and 227°C for the corresponding samarium compound. The stronger separation of the dehydration steps seems to be important for the preparation of the monohydrates. While the latter could not be isolated for M=Pr, the respective samarium compound was obtained, even as single crystals. The decomposition of $Sm(NH_2SO_3)_3$ seems to follow a different mechanism than that of the respective praseodymium compound. The first exothermic step is accompanied by a mass loss of only 16.3% (24.8% for Pr) and the second step, which is now endothermic, is correlated to a mass loss of 13.6% (5.6% for Pr).

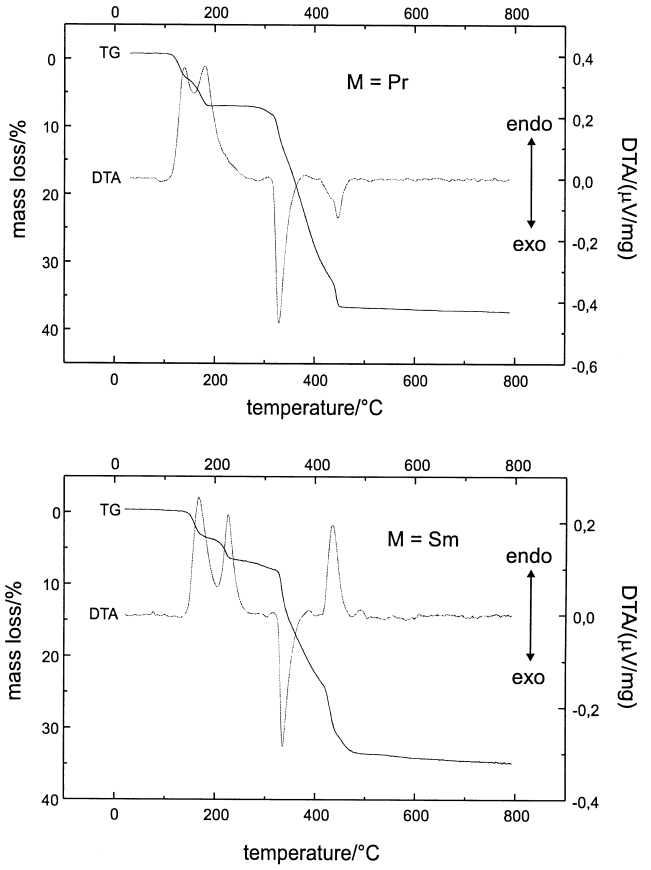

Fig. 4. DTA/TG investigations of the thermal decomposition of $Pr(NH_2SO_3)_3 \cdot 2H_2O$ and $Sm(NH_2SO_3)_3 \cdot 2H_2O$; the respective data are given in the Tables 7 and 8.

The DTA/TG data were confirmed by temperature-dependent X-ray powder diffraction investigations. The diffraction pattern of $Pr(NH_2SO_3)_3 \cdot 2H_2O$ is still observed at 100°C but has completely turned into the one characteristic of $Pr(NH_2SO_3)_3$ at 150°C (Fig. 5). The latter could be indexed based on the single crystal data of $La(NH_2SO_3)_3$ [11] and remains until 400°C when a different diffractogram was recorded. However, because of its poor quality, it could be not indexed unambiguously. This new phase decomposes with further heating, yielding $Pr_2(SO_4)_3$ at 500°C. Refinement of the lattice constants for $Pr_2(SO_4)_3$ was possible using the data of $Nd_2(SO_4)_3$ [12]. For $Sm(NH_2SO_3)_3 \cdot 2H_2O$ the monohydrate intermediate can be seen in the X-ray results (Fig. 6). It occurs at 150°C and was identified with the help of the single crystal data. Reflections of $Sm(NH_2SO_3)_3$ were observed at 200 and 250°C, respectively. The next decomposition step yielded a

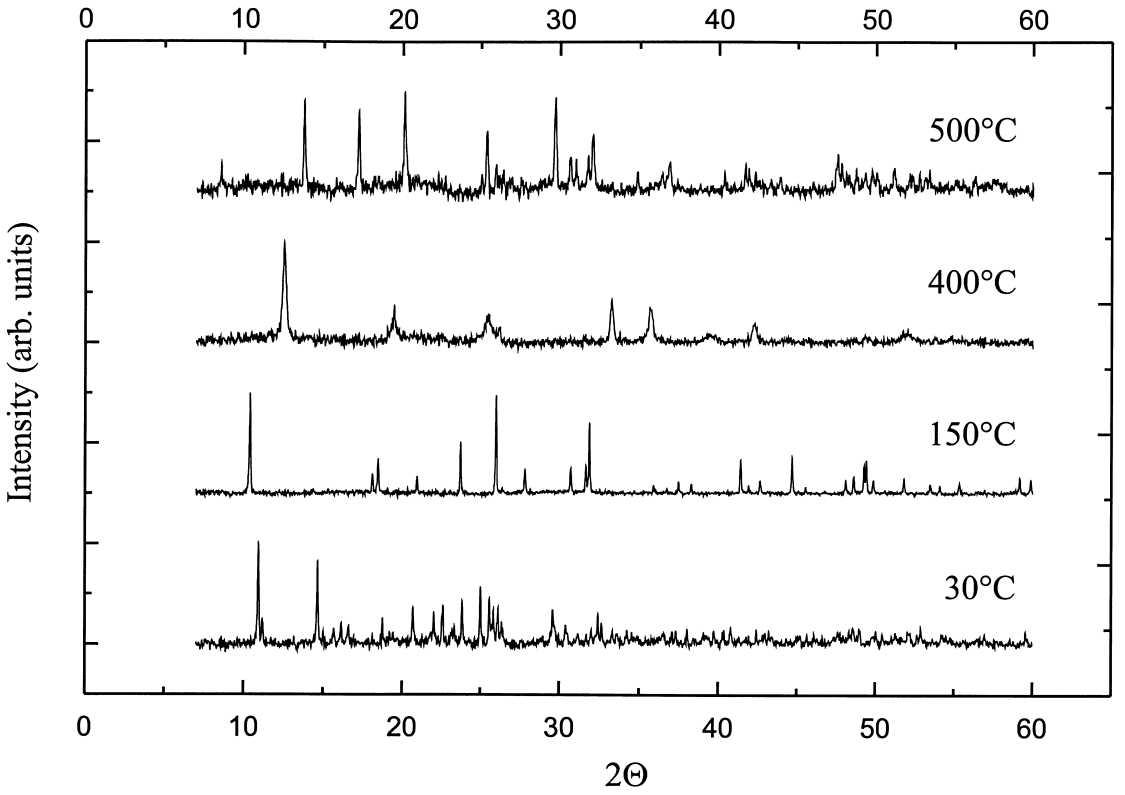

Fig. 5. High temperature X-ray investigations on the thermal decomposition of $Pr(NH_2SO_3)_3 \cdot 2H_2O$ (see also Table 9).

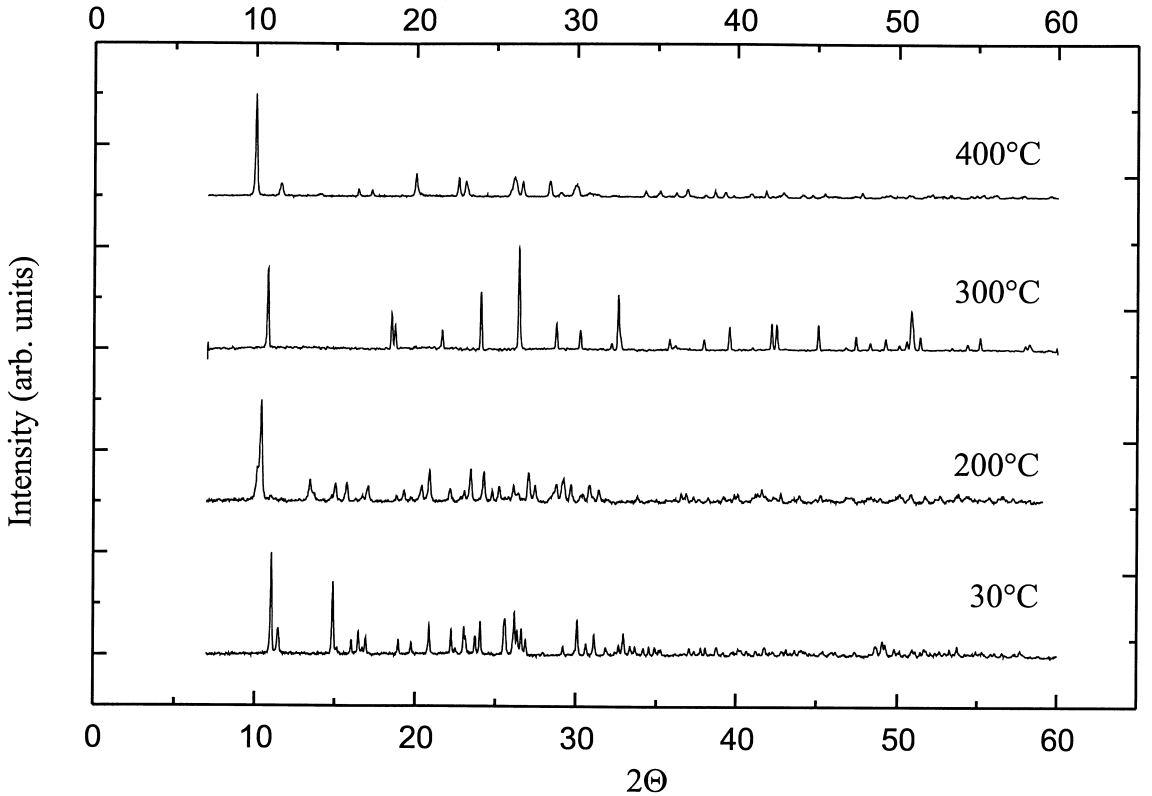

Fig. 6. High temperature X-ray investigations on the thermal decomposition of $Sm(NH_2SO_3)_3 \cdot 2H_2O$ (see also Table 10).

Table 9
Results of the thermal decomposition of $Pr(NH_2SO_3)_3 \cdot 2H_2O$ (X-ray powder data)

T (°C)	Compound	Space group	a (Å)	b (Å)	c (Å)	α (°)	β (°)	γ (°)
30	$Pr(NH_2SO_3)_3 \cdot 2H_2O$	*P-1*	7.912(2)	9.144(1)	9.260(2)	117.44(1)	95.16(2)	92.20(2)
100	$Pr(NH_2SO_3)_3 \cdot 2H_2O$	*P-1*	7.939(2)	9.168(3)	9.264(2)	117.64(3)	95.24(2)	92.33(4)
150	$Pr(NH_2SO_3)_3$	$P6_3/m$	9.7770(6)		5.8156(4)			
200	$Pr(NH_2SO_3)_3$	$P6_3/m$	9.7957(6)		5.8204(4)			
250	$Pr(NH_2SO_3)_3$	$P6_3/m$	9.8130(8)		5.8222(5)			
450	$Pr_2(SO_4)_3$	*C2/c*	21.925(7)	6.739(1)	6.939(2)		110.13(3)	

Table 10
Results of the thermal decomposition of $Sm(NH_2SO_3)_3 \cdot 2H_2O$ (X-ray powder data)

T (°C)	Compound	Space group	a (Å)	b (Å)	c (Å)	α (°)	β (°)	γ (°)
30	$Sm(NH_2SO_3)_3 \cdot 2H_2O$	*P-1*	7.842(2)	9.077(2)	9.202(2)	117.52(2)	95.13(2)	92.21(2)
100	$Sm(NH_2SO_3)_3 \cdot 2H_2O$	*P-1*	7.878(2)	9.104(2)	9.214(3)	117.56(3)	95.14(2)	92.25(2)
150	$Sm(NH_2SO_3)_3 \cdot H_2O$	*P-1*	6.836(3)	9.406(4)	9.452(4)	68.1(4)	75.3(5)	83.5(4)
200	$Sm(NH_2SO_3)_3$	$P6_3/m$	9.7232(8)		5.7768(5)			
250	$Sm(NH_2SO_3)_3$	$P6_3/m$	9.7304(8)		5.7014(4)			
450	$Sm_2(SO_4)_3$	*C2/c*	21.474(4)	6.632(1)	6.863(2)		110.6(2)	

new phase which exhibits a completely different diffraction pattern from that of the praseodymium compound. Finally, the anhydrous sulfate is seen again. The lattice parameters refined from the diffraction data are summarized in Tables 9 and 10, respectively.

Unfortunately, the intermediates of the amidosulfate decomposition were not isolated in single crystal form, so that the decomposition reactions cannot be formulated in detail. According to the present knowledge, however, they may be represented as follows:

$$M(NH_2SO_3)_3 \cdot 2H_2O \underset{-H_2O}{\rightarrow} M(NH_2SO_3)_3 \cdot H_2O \quad (1)$$

$$M(NH_2SO_3)_3 \cdot H_2O \underset{-H_2O}{\rightarrow} M(NH_2SO_3)_3 \quad (2)$$

$$M(NH_2SO_3)_3 \underset{(-2NH_3\ -1/2N_2\ -3/2SO_2)}{\rightarrow ? \rightarrow} 1/2\, M_2(SO_4)_3 \quad (3/4)$$

4. Conclusion

It has been shown that the thermal decomposition of the amidosulfates $M(NH_2SO_3)_3 \cdot 2H_2O$ (M = Pr, Nd, Sm), which have been structurally characterized for the first time, leads to the corresponding anhydrous compounds via monohydrates as intermediates. Furthermore, the decomposition temperatures obtained by DTA/TG and temperature-dependent X-ray measurements were used for the synthesis of the intermediate $Sm(NH_2SO_3)_3 \cdot H_2O$ in single crystal form by slow dehydration of $Sm(NH_2SO_3)_3 \cdot 2H_2O$. Future work will show, whether dehydration reactions can be in general used to grow single crystals which are hard to get by other methods. In particular, such a procedure would be helpful to obtain single crystals of anhydrous lanthanide compounds with complex anions. Note that the crystal structures of anhydrous nitrates, chlorates or carbonates of the rare earth elements are still not known.

Acknowledgements

I am indebted to Prof. Dr. G. Meyer and to the Fonds der Chemischen Industrie, Frankfurt am Main, for generous support. The technical assistance of Mrs. I. Müller is also gratefully acknowledged.

References

[1] M.S. Wickleder, Z. Anorg. Allg. Chem. 625 (1999) 11.
[2] M.S. Wickleder, Z. Anorg. Allg. Chem. 625 (1999) 1556.
[3] C. Belin, F. Favier, J.L. Pascal, M. Thillard-Charbonnel, Acta Crystallogr. C52 (1996) 1872.
[4] M.S. Wickleder, Z. Anorg. Allg. Chem. 624 (1998) 1583.
[5] M. Capestan, Annales De Chimie (1960) 207.
[6] G.M. Sheldrick, SHELXS-86, Programm zur Röntgenstrukturanalyse, Göttingen, 1986.
[7] G.M. Sheldrick, SHELXL-93, Program for the Refinement of Crystal Structures, Göttingen, 1993.
[8] N. Walker, D. Stuart, Acta Crystallogr. A39 (1983) 158.
[9] Netzsch GmbH, Thermal Analysis for the Analyzer STA 409, version 3.1, Selb, 1996.
[10] Stoe and Cie GmbH, VISUAL X-POW 3.01, Software Package for the Stoe Powder Diffraction System, Darmstadt, 1996.
[11] M.S. Wickleder, Z. Anorg. Allg. Chem. 625 (1999) 1794.
[12] S.P. Sirotinkin, V.A. Efremov, L.M. Kovba, A.N. Pokrovskii, Sov. Phys. Crystallogr. 22 (1977) 725.
[13] R.X. Fischer, E. Tillmanns, Acta Crystallogr. C44 (1988) 775.